Monatshefte für Chemie 118, 277—300 (1987)

Monatshefte für Chemie
Chemical Monthly

Thermodynamic Properties and Phase Equilibria of the Lead-Tellurium Binary System*

T. Leo Ngai, D. Marshall, R. C. Sharma***, and Y. A. Chang**

Department of Metallurgical and Mineral Engineering, University of Wisconsin, Madison, WI 53706, U.S.A.

(Received 22 August 1986. Accepted 14 September 1986)

The liquidus curve of the Pb—Te binary was measured using two different DTA systems, one employing a small sample (0.2 g) and the second a large sample (5 g). An additional liquidus measurement method was employed for the Pb-rich region in which the liquid equilibrated with PbTe was analyzed chemically. The liquidus for the Pb—PbTe subsystem obtained is in agreement with several sets of data reported in the literature. The literature data for the PbTe—Te are in disagreement. Our measured values resolve this discrepancy and yield a eutectic temperature of 410.9 ± 0.8 °C at 89.1 ± 0.3 at % Te. The system was thermochemically modelled using an associated solution model for the liquid phase and a defect model for PbTe. This model not only accounts for compositional and temperature dependences of the thermodynamic data but also for electron and hole concentrations within the homogeneous range of PbTe(*c*).

(Keywords: Thermodynamics; Phase equilibria; Lead-tellurium binary)

Thermodynamische Eigenschaften und Phasengleichgewichte des binären Systems Blei—Tellur

Die Liquiduskurve des Binärsystems Pb—Te wurde unter Verwendung von zwei verschiedenen DTA-Systemen (eines unter Anwendung kleiner Probenmengen von 0.2 g, das zweite für größere Probenmengen von 5 g) gemessen. Eine weitere Meßmethode wurde für die Pb-reiche Region herangezogen, wobei die mit Pb—Te äquilibrierte flüssige Phase chemisch analysiert wurde. Der erhaltene Liquidusverlauf für das Pb—PbTe-Subsystem ist mit verschiedenen Literaturdaten in Übereinstimmung. Die Literaturdaten für PbTe—Te sind allerdings abweichend. Unsere Meßdaten klären diese unterschiedlichen Angaben und ergeben eine eutektische Temperatur von 410.9 ± 0.8 °C bei 89.1 ± 0.3 at% Te.

* This paper is dedicated to Prof. Dr. *Kurt L. Komarek* on the occasion of his 60th birthday.

** With Johnson Controls, Inc., Milwaukee, WI 53201, U.S.A.

*** On leave from India Institute of Technology-Kanpur, Kanpur, India.

Für das System wurde ein thermochemisches Modell unter Verwendung eines assoziierten Lösungsmodells für die flüssige Phase und eines Defektmodells für PbTe angewandt. Dieses Modell gab nicht nur die Zusammensetzungs- und Strukturabhängigkeiten der thermodynamischen Daten wieder, sondern auch die Elektronen- und Lückenkonzentrationen innerhalb des homogenen PbTe(*c*)-Bereichs.

1.0 Introduction

As a part of a program to investigate the thermodynamic properties and phase equilibria of multi-component compound semiconductors from groups IV and VI elements, experimental measurements were obtained on the phase equilibria of the important Pb—Te binary. The liquidus for the binary has been determined by *Fay* and *Gillson* [1], *Pelabon* [2], *Kimura* [3], *Gravemann* and *Wallbaum* [4], *Pelzel* [5], *Davey* [6], *Lugscheider* et al. [7], *Miller* and *Komarek* [8], *Wagner* and *Thompson* [9], *Harris* et al. [10], *Moniri* and *Petot* [11], *Astles* et al. [12], *Petukhov* et al. [13], *Kharif* et al. [14], and *Glazer* and *Pavlova* [15]. While the data reported by several groups of investigators for the liquidus from Pb to PbTe are in agreement, this is not true for the liquidus from PbTe to Te. In fact, the PbTe—Te eutectic temperature and composition have not been determined with a high degree of accuracy. The intermediate phase, PbTe, has also attracted many investigations because of its potential applications in infrared detection, both as sensors of thermal radiation and as wide-band detectors in the emerging area of laser radar and laser communications. The large range of homogeneity for PbTe based on earlier studies [1, 16–18] was shown to be in error by more recent investigations [19–22]. In fact, the range of homogeneity is so small it cannot be determined by standard metallographic techniques [21]. *Dedgkaev* et al. [23] determined that PbTe melts congruently at 50.014 at% Te. The exact range of homogeneity for the intermediate phase was obtained from experimentally determined sign and charge carrier concentrations assuming that the non-stoichiometry is caused by the presence of fully ionized vacancies on the Pb and Te sublattices. These measurements for PbTe were carried out by *Brebrick* and *Allgaier* [20], *Fritts* [24], *Brebrick* and *Gubner* [25], *Chou* et al. [21], *Hewes* et al. [26], and *Strauss* [27]. Using these data, several groups of investigators have computed the compositional stability of PbTe [20, 22, 28–30].

Enthalpies of mixing for the liquid phase were determined by *Castanet* et al. [31] at 737 K, *Maekawa* et al. [32] at 736 K, *Moniri* and *Petot* [11] at 879 K and *Blachnik* and *Gather* [33] at 1 210 K. There is agreement among these data within the uncertainties of the measurements. The partial *Gibbs* energies of Te at 1 277 K were measured by *Predel* et al. [34] while those of Pb at 1 123 K were measured by *Fuglevicz* [35]. These data are at variance

with each other. The partial *Gibbs* energies of both Pb and Te were measured in the liquid + PbTe two-phase fields by several groups of investigators [36–43]. Likewise, heat content, enthalpy of melting and enthalpy of formation of PbTe were also determined in several investigations [31, 44–51]. The *Gibbs* energy of formation of PbTe was determined by *McAteer* and *Seltz* [52], *Sadykov* et al. [41], *Shamsuddin* [42], and *Shamsuddin* and *Misra* [53]. Most of these data and the vapor pressure data of PbTe(*g*) in equilibrium with PbTe(*c*) reported by *Pashinkin* and *Novoselova* [54], *Brebrick* and *Strauss* [37] and *Sokolov* et al. [55] were assessed by *Mills* [56]. Within the narrow homogeneous range of PbTe, *Fujimoto* and *Sato* [36] and *Gas'kov* et al. [39] also measured the partial pressure of Te_2 in equilibrium with PbTe. The pressure-temperature-composition (*P-T-X*) data were analyzed in terms of a defect model.

Phase diagram calculations of Pb—Te were carried out by *Laugier* [57], *Laugier* and *Cadoz* [58], *Szapiro* et al. [59] and *Kharif* et al. [14]. An associated solution model was used to describe the liquid phase, and PbTe was treated as a line compound. More recently *Kattner* et al. [60] assessed the entire system using an associated solution model for the liquid phase and a *Wagner-Shottky* model for PbTe. They used a structural defect model for the PbTe phase, but neglected mixing of the electrons due to ionization of vacancies.

The objectives of this study were (1) to determine the liquidus of the PbTe—Te subsystem and the PbTe—Te eutectic temperature and composition and (2) to model the entire system thermochemically using the new experimental data and those reported in the literature as given above. As was done previously [57–60], an associated solution model was used to account for the thermodynamic properties of the liquid phase. For the semiconducting phase, PbTe, a defect model was used. The resulting thermochemical model of this system not only yields a set of consistent thermodynamic values of the various phases but also provides reliable *T-P-X* data for PbTe which would be extremely useful for controlled crystal growth of this compound semiconductor.

2.0 Experimental Method

Two methods were used to measure the liquidus temperatures. The DTA method was used for tellurium concentrations in excess of 3 at%. For compositions containing $\leqslant 3$ at% Te, the composition of a liquid phase in equilibrium with PbTe at a specific temperature was analyzed chemically.

In order to reinforce the reliability of the DTA results, two different apparatus were used; a commercial Perkin-Elmer unit using a small sample (0.2 g) and a home-made unit using a large sample (5 g). The Perkin-Elmer DTA 1700 unit consists of a basic high-temperature differential thermal analyzer, a micropro-

cessor temperature programmer, a thermal analysis data station, and a graphics plotter. This entire unit allows us to carry out DTA experiments either manually or automatically at any desired heating or cooling rate. Each sample, weighing about 0.2 g, was contained in an evacuated quartz tube 3 mm ID, 4 mm OD and approximately 20 mm in height. The reference container was made from a quartz tube with the same dimensions and filled with Al_2O_3 of approximately the same mass. The data were obtained at heating rates of 6, 4 and 2 °C/min and were extrapolated to zero heating rate in order to obtain the liquidus temperatures or the invariant points. The DTA system was calibrated using the IPTS-68 melting points of In, Pb, Te, Sb, Ag and Au with a precision of $\pm$ 1 °C. But the accuracy is estimated to be $\pm$ 1 °C for the low-temperature range and $\pm$ 2 °C for the high-temperature range.

The DTA employing a large sample was constructed at Johnson Controls, Inc., Milwaukee, Wisconsin. Each sample weighing about 5 g was contained in a quartz tube of 8 mm ID, 10 mm OD and 50 mm in height. The tube was evacuated and backfilled several times and finally evacuated to fill with argon to a maximum pressure of 10 Torr and sealed. Each sample was homogenized at 1 150 °C for four hours before carrying out DTA measurements. The reference container was made of a quartz tube with the same dimensions as the sample tube, and filled with Al_2O_3 of the same mass as the sample. Heating rates varied from 4.5 to 0.7 °C/min. This DTA system was calibrated using IPTS-68 melting points of Pb, Ag and Cu with a precision of $\pm$ 1.5 °C. Again, the accuracy is estimated to be $\pm$ 2 °C at high temperatures.

For samples containing less than 3 at% Te, an aliquot method was used to determine the location of the liquidus. This portion of the study was also carried out at Johnson Controls, Inc. Approximately 300 g of COMINCO AMERICAN pure lead, minimum 5-9's purity, was placed in a high purity (Grade 580) graphite crucible made by Helwig Carbon, Inc., Milwaukee, Wisconsin. Curcible dimensions were 4.5 cm ID × 5.1 cm OD × 6.4 cm high. To this was added sufficient tellurium shot (ALFA Products, minimum 6-9's, Cat. No. 00692) to give an overall composition of about 3 at% Te. The crucible and its contents were then placed in a quartz glass vessel to which was fitted an O-ring seal coupling containing appropriate gas connections. A melt was established under a continuous, slow flow of 99.998% argon gas and at a temperature well above the liquidus. Melt temperature was monitored with a thermocouple contained in a quartz glass well. The portion of the thermocouple well contained in the melt had a small paddle fused to it which facilitated melt stirring. The melt was stirred periodically over a three hour period to insure that all the tellurium was in solution.

Following melt formation, the crucible temperature was lowered to a point estimated to be somewhat below the liquidus. During cool-down to the lower temperature, a Pyrex tube (2 mm ID × 4 mm OD, both ends open) was inserted through an O-ring seal at the top of the apparatus and lowered to a position about one centimeter above the melt. With the upper end of the tube connected to an argon line, the tube was purged just before insertion to minimize air entry into the vessel. Once the melt temperature had reasonably stabilized, the Pyrex tube was lowered in increments into the melt while maintaining a positive pressure inside the tube to prevent crystals of PbTe near the top of the melt from entering the tube. The pre-heat time above the melt and gradual insertion reduce the tendency for PbTe to nucleate on the tube. The tube was inserted to a point about one-half centimeter off the bottom of the crucible and the whole apparatus was allowed to equilibrate with periodic stirring.

Once equilibrated, a partial vacuum was applied to the top of the Pyrex tube, forcing an aliquot of the melt phase up the tube. Being substantially cooler above the melt, the aliquot in the tube froze quickly, so the vacuum must be applied rapidly. The tube was then withdrawn from the apparatus, but gradually enough to allow for cooling so as not to damage the O-ring seal. A new tube was then inserted as above and the temperature lowered to establish a new equilibrium. The process was repeated several times for a given melt.

At temperatures sufficiently below the liquidus of the bulk melt, the amount of primary crystallisation may become excessive. This can make it difficult to insert the aliquot tube in the melt, or it can increase the tendency for a primary crystal to enter the tube and be "counted" in the chemical analysis of the liquid phase. Such effects are apparent as a slope change on a graph of log composition vs. $1/T$. Where this was encountered, a new melt was prepared by diluting the original melt with lead.

The Pyrex glass was removed from the aliquot samples by either mechanical or chemical means. For the latter, the glass was dissolved off with HF. To minimize the risk of an extraneous primary crystal influencing the chemical analysis, the top and bottom two centimeters of the sample were cut off. The remainder of the sample was then dissolved in nitric acid for analysis on an Inductively Coupled Plasma (ICP) Emission Spectrograph. Sample tellurium levels were measured along with internal working reference materials prepared from PbO which was spiked with a known quantity of tellurium. The resulting tellurium values for the aliquot samples have a relative accuracy of $\pm$ 10% or less of the amount present.

3.0 Experimental Results

The experimental results are given in Table 1 A and 1 B and shown in Figs. 1 and 2. The results obtained by the two DTA techniques and the aliquot technique (identified as ICP on Figs. 1 and 2) are in agreement with one another. As shown in Figs. 1 and 2, our data from Pb to PbTe are in agreement with the data of *Kimura* [3], *Miller* and *Komarek* [8], *Moniri* and *Petot* [11], *Davey* [6], *Harris* et al. [10], and *Petokhov* et al. [7]. The

Table 1 A. *Experimental results for the liquidus from* Pb *to* PbTe

x_{Te}	T_l (°C)		x_{Te}	T(°C)	
0.0015	352.5	ICP	0.051	638.1	Perkin-Elmer 1700
0.0019	368.9	ICP	0.179	757.7	
0.0021	375.1	ICP	0.292	812.5	
0.0044	418.6	ICP	0.301	813.2	
0.0055	433.4	ICP	0.10	685	Johnson Controls, Inc.
0.0062	445.0	ICP	0.15	735	
0.0115	489.0	ICP	0.25	793	
0.0112	493.2	ICP	0.35	838	
0.0205	539.4	ICP	0.40	867	
0.0233	556.3	ICP	0.45	914	

Table 1 B. *Experimental results for the liquidus from* PbTe *to* Te

x_{Te}	$T_{eutectic}$ (°C)	$T_{liquidus}$ (°C)
0.6006	410.9	845.0
0.6455	412.1	783.7
0.6720	410.2	741.9
0.6989	411.4	715.4
0.7202	411.3	681.7
0.7610	410.1	619.8
0.7851	412.3	592.8
0.8300	411.4	524.3
0.8457	409.5	496.7
0.8750	410.2	—
0.9003	410.5	—
0.9105	411.2	—
0.9252	410.9	425.9
0.9501	410.7	433.8
0.9722	410.3	441.4

Avg. $T_{eutectic} = 410.9 \pm 0.8$ °C

Table 1 C. *Experimental results for the* PbTe—Te *eutectic*

x_{Te}	Primary Phase of Solidification
0.8543	PbTe
0.8648	PbTe
0.8748	PbTe
0.8835	PbTe
0.8892	PbTe
0.8903	PbTe
0.8930	(Te)
0.8966	(Te)
0.8982	(Te)
0.9005	(Te)
0.9026	(Te)
0.9069	(Te)

data of *Lugscheider* et al. [7] are too low in temperature between 10 and 30 at% Te (Fig. 1) while those of *Pelzel* are too high (Fig. 2). From PbTe to Te, our data are in general agreement with those of *Moriri* and *Petot* [11] and *Lugscheider* et al. [7] although one data point of the latter study seems too low in temperature. It is also evident from Fig. 1 that previous data do

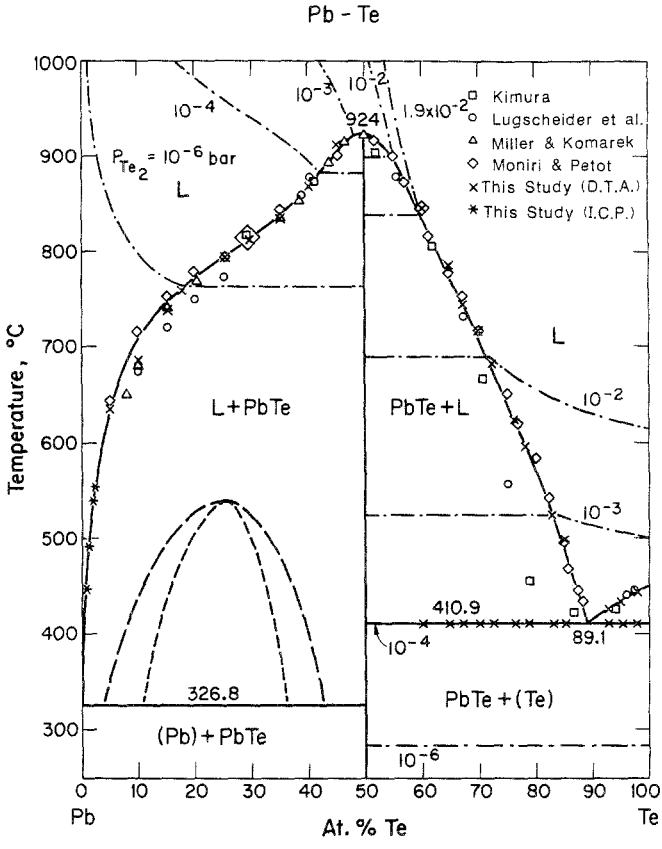

Fig. 1. The Pb—Te phase diagram: comparison between the experimental data obtained in the present study with those reported in the literature, and comparison between the experimental data with the calculated diagram

not adequately resolve the PbTe—Te eutectic temperature and composition. We have carried out DTA measurements on numerous samples (Fig. 1) and have determined the average and standard deviation for the eutectic temperature to be 410.9 ± 0.8 °C. The eutectic composition was determined metallographically as given in Table 1 C. These samples were held at 600 °C for one hour and furnace cooled to room temperature for metallography. On the basis of these examinations, the eutectic composition was determined to be 89.1 ± 0.3 at% Te. DTA results for three Te-rich alloys with 99.5, 99.0 and 97.5 at% Te showed thermal arrest at ~ 411 °C upon heating. These results suggest negligible solubility of Pb in Te(*c*).

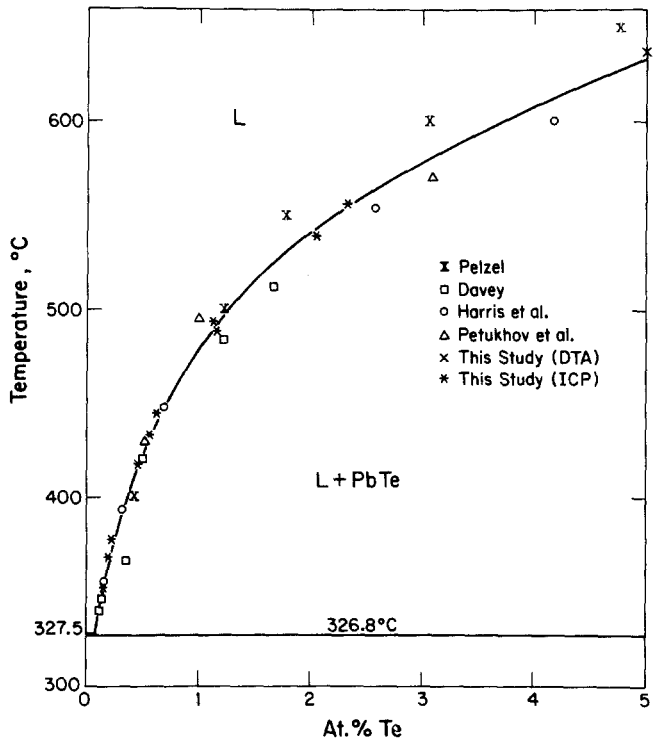

Fig. 2. The lead-rich Pb—Te phase diagram: comparison between the experimental data obtained in the present study with those reported in the literature, and comparison between the experimental data with the calculated diagram

4.0 Analysis of the Data

4.1 Thermodynamic Models

4.1.1 The Liquid Phase

An associated solution model [61–65] was used to describe the thermodynamic properties of the liquid phase in the Pb—Te system. According to this model, the liquid Pb—Te phase is assumed to consist of "Pb", "Te" and "PbTe" species in the liquid, governed by the following equilibrium:

$$\text{"Pb"}(l) + \text{"Te"}(l) = \text{"PbTe"}(l) \tag{1}$$

with an equilibrium constant given by:

$$K = \frac{f_3 y_3}{(f_1 y_1)(f_2 y_2)} \tag{1 A}$$

where f_1, f_2 and f_3 are the activity coefficients and y_1, y_2 and y_3 are the mole fractions of "Pb", "Te" and "PbTe", respectively in the liquid. The mole fractions, y_i's, are related to the actual mole fractions, x_{Pb} and x_{Te} of Pb and Te, respectively, by the following mass balance equations:

$$y_1 = x_{Pb} - x_{Te}\, y_3 \tag{2}$$

and

$$y_2 = x_S - x_{Pb}\, y_3 \tag{3}$$

The activity coefficients, f_i's, are described by a *Margules* type equation as given below [66, 67]:

$$\ln f_i = \sum_{j=1}^{n} [(w_{ij} + w_{ji})/2 + (w_{ij} - w_{ji})(y_j/2 - y_i)]\, y_j - \sum_{j=1}^{n} \sum_{p=1}^{n} [w_{jp}/2 - (w_{jp} - w_{pj})\, y_j]\, y_j\, y_p \tag{4}$$

where i, j and p vary from 1 to 3, and w_{ij}, w_{ji} are the interaction parameters of the solutions, with $w_{ii} = w_{jj} = 0$. The interaction parameters are represented as

$$w_{ij} = A_{ij}/T + B_{ij} \tag{5}$$

with A_{ij} and B_{ij}, being constants whose values must be obtained from experimental data. The activities of "Pb" and "Te" species are

$$a_1 = f_1\, y_1 \tag{6 A}$$

and

$$a_2 = f_2\, y_2 \tag{6 B}$$

with Pb(l) and Te(l) as the standard states. Since the activities of the "Pb" and "Te" species are the same as those of the Pb and Te components [68], we have the following equations:

$$a_1 = f_1\, y_1 = a_{Pb} = \gamma_{Pb}\, x_{Pb} \tag{7}$$

and

$$a_2 = f_2\, y_2 = a_{Te} = \gamma_{Te}\, x_{Te} \tag{8}$$

where γ_{Pb} and γ_{Te} are the activity coefficients of Pb and Te which differ from f_1 and f_2. Values for the various parameters may be obtained using available thermodynamic and phase equlibria data.

Although the associated solution model is able to account for the compositional dependence of the thermodynamic properties of the Pb—Te melts from pure Pb to Te, it is cumbersome to use for numerical computation without the aid of a computer. Since some of the practical

calculations involve dilute solutions we have used the interaction parameters introduced by *Wagner* [65, 69]. The relationships between $\ln \gamma_2^0$, ε_2^2 and ρ_2^2 and the parameters of the solution models are given below where x_2 approaches zero.

$$\ln \gamma_2^0 = w_{31} - \ln K \tag{9}$$

$$\varepsilon_2^2 = 2(1 + w_{13} - 2w_{31}) \tag{10}$$

$$\rho_2^2 = 2 - w_{13} - w_{31} \tag{11}$$

The term γ_2^0 is the activity coefficient of Te at infinite dilution, ε_2^2 is the self-interaction parameter of Te and ρ_2^2 is the second-order self-interaction parameter of Te. Conversions of ε_2^2 and ρ_2^2 to e_2^2 and r_2^2 in terms of wt% and logarithm to the base 10 may be made using the formulas given by *Lupis* and *Elliott* [69].

4.1.2 The PbTe Phase

Since the stability range of PbTe is very narrow, it may be considered as a stoichiometric compound for the purpose of calculating the liquidus in equilibrium with PbTe. Its *Gibbs* energy of formation from pure Pb(l) and $Te_2(g)$ can be expressed as a linear function of temperature

$$\Delta G_f^0 = C + DT \tag{12}$$

where C and D are contents.

The PbTe phase, however, does have slight deviations from stoichiometry which affect its semiconducting properties. The model developed by *Lin* et al. [70] has been used here to describe the thermodynamic properties of this phase as a function of composition. According to this model, doubly ionized vacancies exist on the Pb and Te-sublattice in the PbTe phase. At the stoichiometric composition, the concentration of vacancies on either sublattice is equal to the concentration of vacancies on the other sublattice. An excess of vacancies on the Te-sublattice gives a Pb-rich phase and vice versa. For small deviations from the stoichiometric composition, the following equilibrium equations may be written [70, 71]:

$$\mathrm{Pb}(g) = [\mathrm{Pb}] + \square_{\mathrm{Te}}^{+2} + 2e^-; \quad K_{\mathrm{Pb}} = \frac{[\square_{\mathrm{Te}}^{+2}]\, n^2}{p_{\mathrm{Pb}}} \tag{13}$$

$$1/2\,\mathrm{Te}_2(g) = [\mathrm{Te}] + \square_{\mathrm{Pb}}^{-2} + 2h^+; \quad K_{\mathrm{Te}} = \frac{[\square_{\mathrm{Pb}}^{-2}]\, p^2}{P_{\mathrm{Te}_2}} \tag{14}$$

and

$$\mathrm{Pb}(g) + 1/2\,\mathrm{Te}_2(g) = \mathrm{PbTe}(c); \quad K_{\mathrm{PbTe}} = \frac{1}{p_{\mathrm{Pb}}\, p_{\mathrm{Te}_2}^{1/2}} \tag{15}$$

where $\square_{Te}^{+2}$ and $\square_{Pb}^{-2}$ refer to the ionized vacancies on the Te-sublattice and Pb-sublattice, respectively, and $[\square_{Te}^{+2}]$ and $[\square_{Pb}^{-2}]$ are their respective concentrations in the PbTe lattice. The quantities e^- and h^+ refer to the free electrons in the conduction band and holes in the valence band, respectively, and n and p are their corresponding concentrations. The term p_{Pb} and p_{Te_2} are the partial pressures of $Pb(g)$ and $Te_2(g)$, respectively, in equilibrium with the PbTe phase. K_{Pb}, K_{Te} and K_{PbTe} are equilibrium constants for the corresponding reactions. Now, for a non-degenerate semiconductor,

$$np = n_i^2 = p_i^2 \tag{16}$$

and also

$$\begin{aligned}[\square_{Te}^{+2}][\square_{Pb}^{-2}] &= K_s = [\square_{Te}^{+2,0}][\square_{Pb}^{-2,0}] \\ &= [\square_{Te}^{+2,0}]^2 = [\square_{Pb}^{-2,0}]^2\end{aligned} \tag{17}$$

where n_i and p_i are the concentrations of electrons and holes, respectively, for the stoichiometric (intrinsic) compound semiconductor PbTe; $[\square_{Te}^{+2,0}]$ and $[\square_{Pb}^{-2,0}]$ are the defect concentrations of vacancies on the Te-sublattice and Pb-sublattice, respectively, for the stoichiometric composition, and K_s is the equilibrium constant. Finally, to maintain the electrical neutrality of the compound, we have:

$$(n - p) + 2([\square_{Pb}^{-2}] - [\square_{Te}^{+2}]) = 0 \tag{18}$$

Now by rearranging and simplifying equations (13) to (18), we obtain [70]

$$\ln p_{Te_2} = \ln p_{Te_2}^0 + 4\,\mathrm{Sinh}^{-1}\left[\frac{p-n}{2n_i}\right] + 2\,\mathrm{Sinh}^{-1}\left[\frac{p-n}{4K_s^{1/2}}\right] \tag{19}$$

where $p_{Te_2}^0$ is the partial pressure of $Te_2(g)$ in equilibrium with stoichiometric PbTe. Based on the theory of non-degenerate semiconductors, *Lin* et al. [70] obtained:

$$\ln n_i = A' + B'/T + 1.5 \ln T \tag{20}$$

where $B' = -E_g^0/2k$, A' is an adjustable parameter, E_g^0 is the energy of band gap at 0 K and k is the *Boltzmann* constant. Furthermore, $\ln K_s$ and $\ln p_{Te_2}^0$ are assumed to vary linearly with reciprocal temperature to give:

$$\ln K_s = E + F/T \tag{21}$$

and

$$\ln p_{Te_2}^0 = G + H/T \tag{22}$$

where E, F, G and H are constants. The composition of the PbTe phase is related to the relative concentrations of vacancies on the two sublattices

and, therefore, also to the relative concentrations of electrons and holes via equation (18), to give:

$$x_{Te} = 0.5 + \frac{(p-n)\,M}{8\,\rho\,N} = 0.5 + \frac{(p-n)}{11.88 \times 10^{22}} \tag{23}$$

where x_{Te} is the atomic fraction of Te in the PbTe phase, n and p are the concentrations of electrons and holes per cm^3, respectively, M and ρ are the molecular weight and density, respectively, of PbTe and N is the *Avogadro*'s number. Equation (19), therefore, gives the equilibrium partial pressure of $Te_2(g)$ over the PbTe phase (or the activity of tellurium) as a function of composition. The activity of Pb may then be obtained from the activity of tellurium and the *Gibbs* energy of formation of the PbTe phase.

4.2 Data Evaluation

4.2.1 The Pure Components

The enthalpies of melting and the melting points for Pb and Te were taken from the literature [72, 73]. The derived *Gibbs* energies of melting are given in Table 2.

4.2.2 The *PbTe* Phase

Using the assessed value of ΔH_f^0 by *Mills* [56] and the *Gibbs* energy functions of PbTe [56], Pb [72] and Te [72], the *Gibbs* energies of formation for PbTe were obtained as given in Table 2A. The enthalpy of melting was obtained by optimizing all the pertinent thermodynamic and phase equilibrium data. The resulting value of 42.0 kJ/mol, as given in Table 2, is in agreement with the measured value of 41.4 ± 1.3 kJ/mol by *Shamsuddin* [42] and *Shamsuddin* and *Misra* [53].

4.2.3 The Liquid Phase

Values of K and w_{ij} given in Table 3 were obtained using the calorimetric data [11, 31–33], the activity data of *Fuglevicz* [35], the

Table 2A. *Thermodynamic data of* Pb, Te *and stoichiometric* PbTe

Phase reactions	ΔG°, J/mol	Refs.
$Pb(c) = Pb(l)$	$4\,799 - 7.99\,T$	[72], [73]
$Te(c) = Te(l)$	$17\,489 - 24.199\,T$	[72], [73]
$Pb(l) + Te(l) = PbTe(c)$	$-95\,193 + 43.30\,T$	this study
$PbTe(c) = PbTe(l)$	$41\,956 - 35.05\,T$	this study

Table 2B. *Thermodynamic data of the* PbTe *phase in terms of deviations from stoichiometry*

$\log n_i = -\frac{468.17}{T} + 14.711 + 1.5 \log T$		this study
$\log K_s^{1/2} = -\frac{6\,223.32}{T} + 24.284$		this study
$\log p^0_{Te_2}(\text{bars}) = -\frac{13\,085.35}{T} + 7.155$		this study
ρ, g/*cc*	8.25	[20]
Z	2	[75], [76]
E_g^0, ev	0.1859	[80], [81]

Table 3. *Thermodynamic data of the liquid phase-subscript 1: the* "Pb" *species, subscript 2: the* "Te" *species, and subscript 3: the* "PbTe" *species*

$$\text{"Pb"}(l) + \text{"Te"}(l) = \text{"PbTe"}(l) \quad K = \left(\frac{y_3}{y_1 y_2}\right)\left(\frac{f_3}{f_1 f_2}\right)$$

$$\ln K = -2.0643 + \frac{7\,417.3}{T} \qquad w_{12} = w_{21} = 0$$

$$w_{13} = 0.0408 + \frac{841.8}{T} \qquad w_{31} = -0.6490 + \frac{2\,344.5}{T}$$

$$w_{23} = -1.7464 + \frac{1\,371.4}{T} \qquad w_{32} = 1.1527 - \frac{1\,613.7}{T}$$

$$\ln \gamma_2^0 = 1.415 - \frac{5\,073}{T}$$

$$\varepsilon_2^2 = 4.677 - \frac{7\,695}{T} \qquad e_2^2 = 0.03025 - \frac{54.22}{T}$$

$$\rho_2^2 = 2.608 - \frac{3\,186}{T} \qquad r_2^2 = 0.01013 - \frac{2.636}{T}$$

$$\text{Pb}(l) + \text{Te}(l) = \text{PbTe}(l) \qquad \Delta G^0 = -53\,237 + 8.25\,T \text{ in J/mol}$$

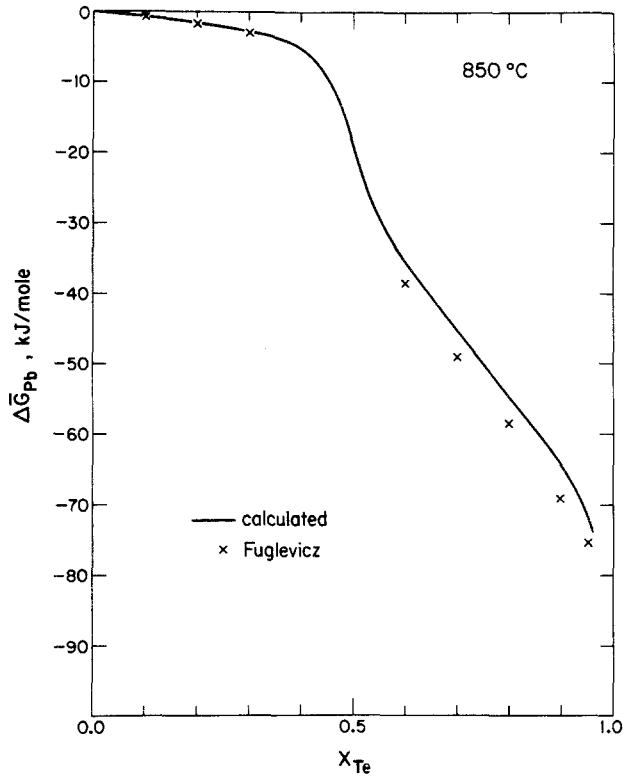

Fig. 3. The partial *Gibbs* energy of Pb at 1 123 K (850 °C): comparison between the experimental data and the calculated values

melting point of PbTe at 924 K [19, 42], the liquidus data obtained in the present study and the agreeing values reported in the literature [3, 6, 8, 10, 11, 13]. The enthalpy of melting was treated as a parameter but was allowed to vary within the uncertainty of the experimental data [42, 53]. As shown in Fig. 3, the calculated values of $\Delta\bar{G}_{Pb}$ are in agreement with the measured values of *Fuglevicz* [35]. The experimental vapor pressure data of *Predel* et al. [34] are high when compared with the calculated values. Fig. 4 shows a comparison of the calculated ΔH values with those of *Blacknik* and *Gather* [33] at 1 210 K. The data of *Constanet* et al. [31], *Maekawa* et al. [32] and *Moniri* and *Petot* [11], which are not shown in this figure, are in agreement with the calculated values and the experimental data of *Castanet* et al. Within the uncertainities of the data, ΔH values are temperature-independent. Fig. 5 provides a comparison between the experimental and calculated entropy values. The experi-

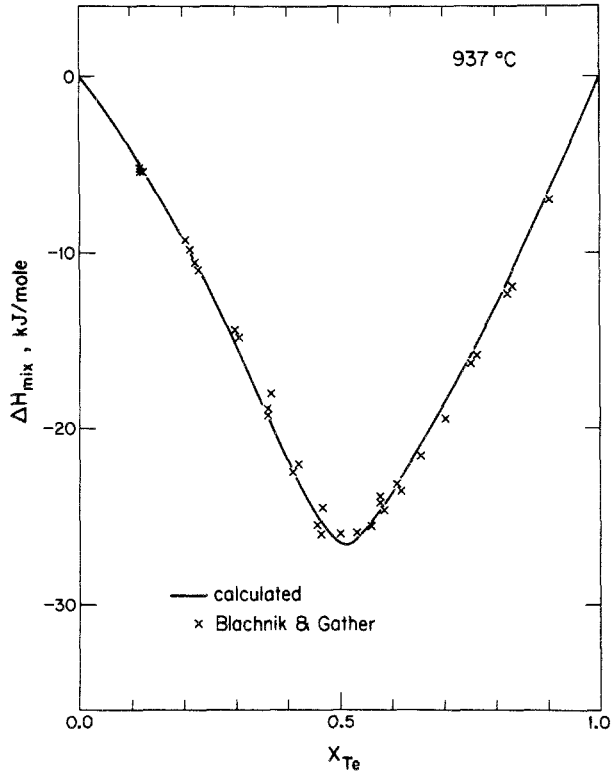

Fig. 4. The enthalpy of formation of the liquid phase at 1 210 K (937 °C): comparison between the experimental data and the calculated values

mental entropy values were obtained using the ΔG values calculated from the model and the ΔH values of *Blacknik* and *Gather* at 937 °C [33].

Using Eqs. (9)–(11) values of $\ln \gamma_2^0$, ε_2^2 and ρ_2^2 were obtained as given in Table 3. Values of e_2^2 and r_2^2, expressed in terms of logarithm to the base 10 and wt%, are also given in the same table [69].

Using the relationships given by *Schmid* and *Chang* [65], values of ΔG_f^0 for the liquid phase at 50 at% Te are also calculated and given in Table 3.

4.3 Phase Diagrams Calculation

The liquidus in equilibrium with PbTe(c) was calculated using the following equation:

$$\Delta \bar{G}_{Pb} + \Delta \bar{G}_{Te} = \Delta G^0_{f,PbTe(c)} \tag{24}$$

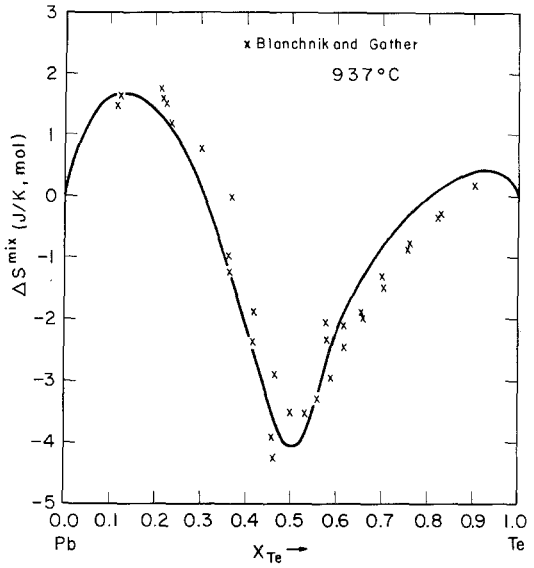

Fig. 5. The entropy of formation of the liquid phase at 1 210 K (937 °C): comparison between experimental data and the calculated values

where $\Delta \bar{G}_{Pb}$ and $\Delta \bar{G}_{Te}$ are the relative partial *Gibbs* energies of Pb and Te for the liquid phase with respect to Pb(l) and Te(l) and $\Delta G^0_{f,PbTe}$ is the *Gibbs* energy of formation of PbTe at the stoichiometric composition also with respect to Pb(l) and Te(l). In calculating the liquidus curves in equilibrium with pure Pb or Te, the solubilities of the minor components are taken to be zero.

The calculated phase diagram as shown in Fig. 1 is in good agreement with the experimental data obtained in the present study and those of *Kimura* [3], *Miller* and *Komarek* [8], and *Moniri* and *Petot* [11]. The data of *Lugscheider* et al. [7] in the mid-composition range are in agreement with other data and the calculated values but they are too low in temperatures elsewhere. Other than our experimental data, the data of *Moniri* and *Petot* [11] are the most extensive between PbTe and Te. The agreement of our data and our calculated values with their study is good. Many of the data reported in the literature (see 2.0) are not plotted in Fig. 2 either because they cover a limited concentration range or deviate significantly from the agreeing data shown in Fig. 1. Also shown as dashed lines in Fig. 1 is a calculated metastable liquid miscibility gap between Pb and PbTe. The short-dashed line represent the calculated spinodal for this metastable miscibility gap.

Comparisons between our experimental and calculated liquidus temperatures for the Pb-rich region and the experimental values reported in the literature are given in Fig. 2. With the exception of *Pelzel*'s data [5], all others are in reasonable agreement with one another.

Our calculated invariant equilibria are compared with the experimental data and those calculated by *Kattner* et al. [60] as given in Table 4.

Table 4. *Comparison between the calculated and experimental invariant equilibria*

T, K	x_{Te}	Refs.
1. The congruent-melting point of PbTe		
1 190	—	[1]
1 177	—	[3]
1 197	0.50002	[19]
—	0.50012	[20]
1 187	—	[7]
1 197	—	[42]
—	0.50014	[23]
1 196	0.5001	[60] (cal'd)
1 197	0.50007	this study (cal'd)
2. The Pb—PbTe-eutectic		
600.0	0.0004	[74]
600.1	0.0010	[60] (cal'd)
600.1	0.00109	this study (cal'd)
3. The PbTe—Te eutectic		
673	0.852	[1]
685	0.837	[3]
651	0.82	[7]
686	0.893	[11]
684.1 ± 1	0.8913 ± 0.003	this study (exp't)
684.3	0.8926	[60] (cal'd)
684.1	0.8913	this study (cal'd)

The calculated value of 1 197 K for the melting point of PbTe agrees with the experimental data of *Shamsuddin* [42] and *Miller* and *Komarek* [19]. The calculated congruent-melting composition of $x_{Te} = 0.50007$ is close to the average value of *Miller* and *Komarek* [19], *Brebrick* and *Allgaier* [20] and *Dedgkaev* et al. [23]. For the Pb—PbTe eutectic, the calculated temperature of 600.1 K is in agreement with that of *Greenwod* and *Warner* [14] but the calculated eutectic composition of $x_{Te} = 0.00109$ is higher than the experimental value. However, in view of the intrinsic experi-

mental difficulty in determining the eutectic composition for a degenerate eutectic, the calculated composition may be more reliable. For the PbTe—Te eutectic, our experimental determination is the most extensive and reliable one as shown in Fig. 1 and Table 1. Our calculated values for the eutectic temperature and composition are in agreement with the experimental results as given in Table 4.

4.4 Discussion

In view of the extremely narrow range of homogeneity for PbTe(*c*), its integral *Gibbs* energy remains essentially constant with composition within the homogeneous range. However, the partial *Gibbs* energies change appreciably even with minute deviations from stoichiometry. In order to calculate the variations of the partial *Gibbs* energy of Te with composition using Eq. (19), we need to know the values of the 5 model parameters, i.e. A', E, F, G and H given in Eqs. (20)–(22). These values are obtained by equating the partial *Gibbs* energies of Pb and Te between PbTe and the liquid phase using known phase boundary and thermodynamic data within the homogeneous field of PbTe. A set of values for these parameters is obtained by optimization as given in Table 2 B (section 4.2.2). The value of B' is obtained from the energy of band gap at 0 K [81, 82]. Fig. 6 shows the calculated phase boundaries of PbTe(*c*) in equilibrium with the liquid phase as compared to the experimental data. The calculated phase boundaries are in agreement with the experimental data of *Fritts* [24] and *Hewes* et al. [26]. The Pb-rich phase boundary data of *Brebrick* and *Gubner* [25] are in agreement with the other two sets of data and our calculated values. But the Te-rich data at high temperatures seem too low in Te concentrations. One plausible explaination for the apparently low Te concentrations obtained by *Brebrick* and *Gubner* [25] is the inability to quench the homogeneous solid solutions to lower temperatures. As shown in Fig. 6, the solubility of Te in PbTe decreases rapidly with decreasing temperature below $\sim 800\,^{\circ}C$. The 5 data points at ~ 800 and $\sim 700\,^{\circ}C$ have essentially the same compositions as those data points at $\sim 600\,^{\circ}C$. This can be readily explained if we cannot quench the single-phase solutions to temperatures below $\sim 600\,^{\circ}C$. The retrograde behavior for the compositional stability of PbTe(*c*) appears to be real. We have analyzed the thermodynamic and phase equilibrium data of several other IV–VI semiconductor compound phases. They all exhibit behavior similar to PbTe(*c*) [77]. The data of *Brebrick* and *Allgaier* [20] are too low in Te concentrations for the Pb-rich phase boundary and too high in Te concentration for the Te-rich phase boundary. Fig. 7 shows a comparison between the calculated stability diagram and the experimental data. With the exception of few data points, the calculated iso-compositional lines are

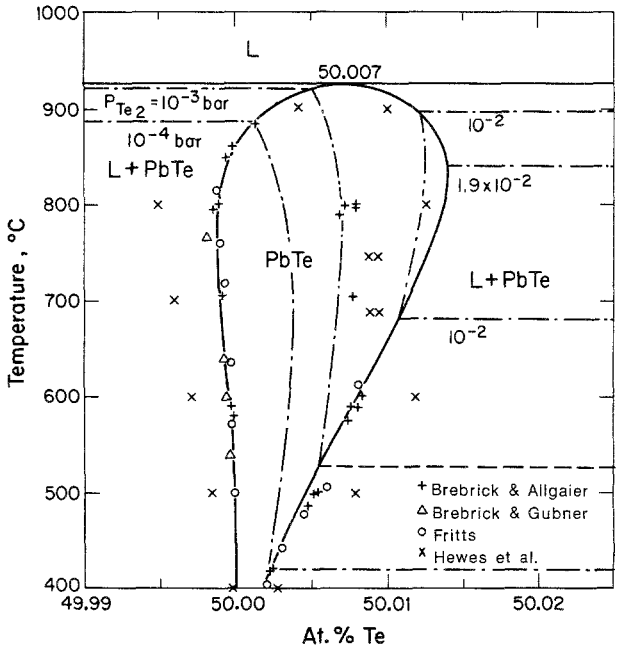

Fig. 6. The Pb—Te phase diagram in the vicinity of PbTe(*c*): comparison between experimental data and the calculated values

in agreement with data of *Fujimoto* and *Sato* [36] and *Gaskov* et al. [29]. Also shown in Fig. 7 are Te_2 partial pressure data of *Bis* [38] and *Brebrick* and *Strauss* [37] in the L + PbTe two-phase fields. Within the uncertainties of the methods, the calculated partial pressure values along the phase boundaries are in agreement with their data. The abrupt change in the slope of *Bis'* data for the Te-rich phase boundary is not easily reconciled.

Although the model used is able to describe the thermodynamic behavior of PbTe, a word of caution should be made. The model was derived assuming non-degenerate semiconducting behavior. The concentrations of electrons and holes as shown in Fig. 7 are somewhat high for this assumption. A more realistic description is to relax this assumption. We are currently working on such a model. But in the meantime, the model as presented is able to describe quantitatively the compositional and temperature dependences for the concentrations of the electrons and holes for PbTe(*c*) and several IV–VI compound semiconductors [76]. It is noteworthy to point out that *Kattner* et al. [60] also modelled the Pb—Te system thermochemically as mentioned earlier.

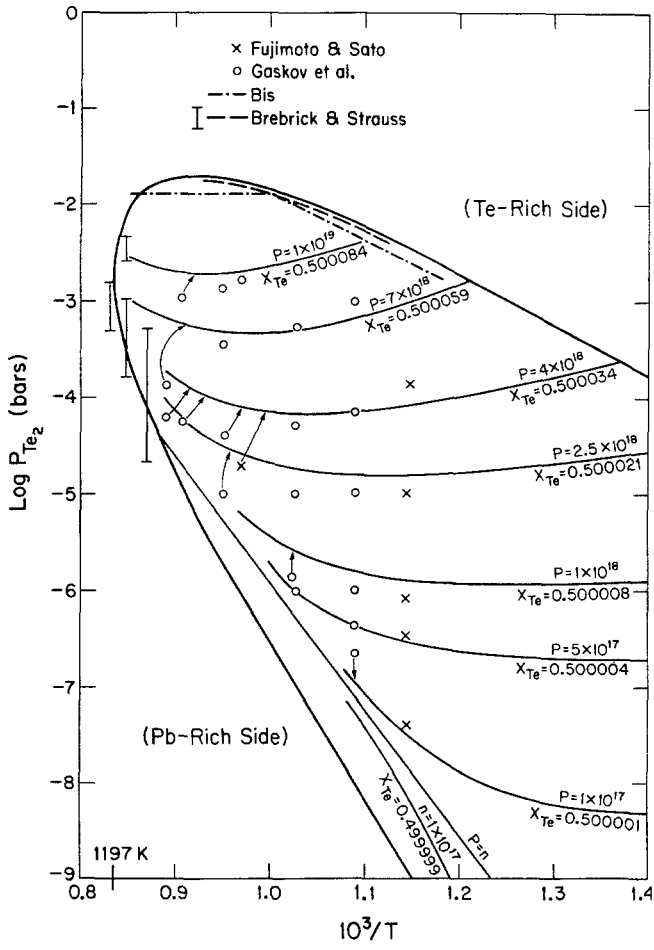

Fig. 7. The stability diagram for PbTe(*c*): comparison between experimental data and the calculated results

Although there is no evidence for the existence of "PbTe" (*l*) in the Pb—Te liquid phase as pointed out previously [64, 65], the associated model is able to describe the thermodynamic properties of this liquid phase from pure Pb to Te. Moreover, we may use this model to calculate the concentration-concentration correlation factor S_{cc} [65]. According to *Bhatia* and *Thornton* [78], the scattering function for binary alloys may be expressed in terms of three structure factors constructed from the *Fourier* transforms of the local number density and concentration in the alloy.

These structure factors are a function of the wavelength used in scattering experiments. In the limit of long wavelength, or zero wave vector, the concentration-concentration correlation function, $S_{cc}(0, x_B, T)$, is related to the mean square thermal fluctuation in concentration, $\langle(\Delta c)^2\rangle$, by

$$S_{cc}(0, x_B, T) = N\langle(\Delta c)^2\rangle \tag{25}$$

where N is the *Avogadro's* number and the concentration is on a mole fraction scale [39]. S_{cc} may be obtained either from extrapolation of x-ray scattering densities to zero wave vector [78] or form activity data via the following relationship [78, 79]:

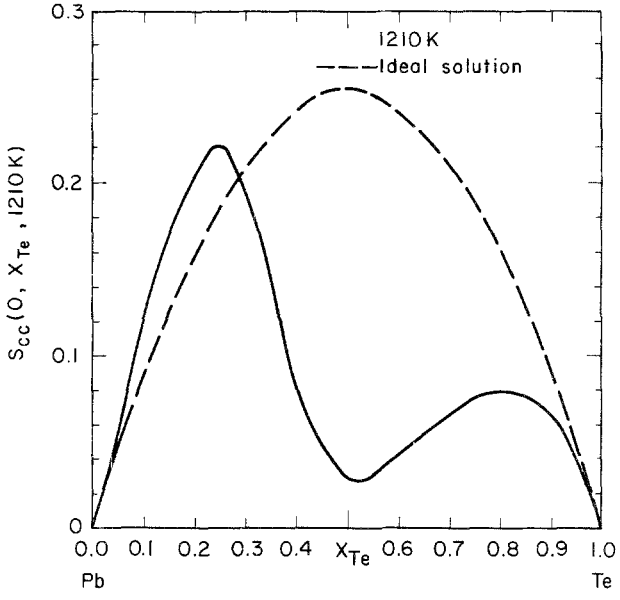

Fig. 8. The concentration-concentration correlation function, S_{cc}, for zero wave vector at 1 210 K indicating the mean square thermal fluctuations as a function of composition in the Pb—Te liquid phase

$$S_{cc}(0, x_B, T) = \frac{RT}{(\partial^2 \Delta G/\partial x_B^2)_T} = \frac{1 - x_B}{(\partial \ln a_B/\partial x_B)_T} \tag{26}$$

For an ideal solution, Eq. (26) reduces to

$$S_{cc}^{id}(0, x_B) = x_B(1 - x_B) \tag{27}$$

Fig. 8 shows the concentration-concentration correlation function $S_{cc}(0, x_{Te}, 1\,273\,K)$ and also $S_{cc}^{id}(0, x_{Te})$ for comparison. As would be

expected, $S_{cc}^{id}(0, x_{Te})$ varies symmetrically with composition and exhibits a maximum at $x_{Te} = 0.5$. $S_{cc}(0, x_{Te}, 1\,273\,K)$ shows a minimum at $x_{Te} = 0.5$ and a pronounced maximum at $x_{Te} = 0.235$. This composition corresponds closely to the critical composition for the metastable liquid miscibility gap as shown in Fig. 1.

5.0 Acknowledgement

The authors wish to thank the National Science Foundation for financial support through Grant Nos. NSF-DMR-83-10529 and NSF-DMR-85-14421, Johnson Controls, Inc. for its support of this research and *J.-C. Lin* for his help in some of the calculation and his comments and criticism.

6.0 References

[1] *Fay H, Gillson CB* (1902) Am Chem J 27: 81–95
[2] *Pelabon MH* (1909) Ann Chim Phys 17: 526–566
[3] *Kimura M* (1915) Mem Coll Sci Kyoto Univ 1: 149–152
[4] *Gravemann H, Wallbaum H-J* (1956) Z Metallk 47: 433–441
[5] *Pelzel BE* (1956) Metall 10: 717–719
[6] *Davey TRA* (1961) Physical chemistry of process metallurgy, AIME. Interscience, New York (AIME metallurgical society conference, vol 7), pp 581–600
[7] *Lugscheider W, Ebel H, Langer G* (1965) Z Metallk 56: 851–852
[8] *Miller E, Komarek KL* (1966) Trans TMS AIME 236: 832–840
[9] *Wagner JW, Thompson AG* (1970) J Electrochem Soc 117: 936–940
[10] *Harris JS, Longo JT, Gertner ER, Clarke JE* (1975) J Cryst Growth 28: 334–342
[11] *Moniri N, Petot C* (1978) J Calorim Anal Thermo (Prepr) 9 B: B 24 195–201
[12] *Astles Poltatto MG, Crocker AJ* (1979) J Cryst Growth 47: 379–383
[13] *Petukhov AP, Andreev YuV, Olesk AO* (1980) Izv Akad Nauk SSSR, Neorg Mater 16: 272–274; *Petukhov AP, Andreev YuV, Olesk AO* (1980) Inorg Mater 16: 176–177
[14] *Kharif YL, Kovtunenko PV, Maier AA, Avetisov IK* (1982) Russ J Phys Chem 56: 1331–1334
[15] *Glazor VM, Parlova LM* (1983) Russ J Phys Chem 57: 1314–1318
[16] *Endo H* (1927) Science Repts Tohoku Imp Univ 16: 201–210
[17] *Honda K, Endo H* (1927) J Inst Metals 37: 29–49
[18] *Hansen M, Anderko K* (1958) Constitution of binary alloys, 2nd ed. McGraw-Hill, New York
[19] *Miller E, Komarek K, Cadoff I* (1959) Trans TMS AIME 215: 882–887
[20] *Brebrick RF, Allgaier RS* (1966) J Chem Phys 32: 1826–1831
[21] *Miller E, Komarek K, Cadoff I* (1960) Trans TMS AIME 218: 382
[22] *Chou N, Komarek K, Miller E* (1969) Trans TMS AIME 245: 1553–1560
[23] *Dedgkaev TT, Mikrousov NE, Moshnikov VA, Taskov DA* (1983) Russ J Phys Chem 57: 944–946
[24] *Fritts RW* (1969) In: *Cadoff IB, Miller E* (eds) Thermoelectric materials and devices. Reinhold, New York, pp 143–162
[25] *Brebrick RF, Gubner E* (1962) J Chem Phys 36: 1283–1289

[26] *Hewes CR, Adler MS, Senturia SD* (1973) J Appl Phys 44: 1327–1332
[27] *Strauss AJ* (1973) J Elec Materials 2: 553–569
[28] *Brebrick RF* (1977) J Electron Mater 6: 659–692
[29] *Gas'kov AM, Zlomanov VP, Novogelova AV* (1979) Inorg Mater 15: 1153–1165
[30] *Akchurin RK, Ufimtsev VB* (1979) Russ J Phys Chem 53: 814–816
[31] *Castanet R, Claire Y, Laffitte M* (1972) High Temp High Press 4: 343–351
[32] *Maekawa T, Yokokawa T, Niwa K* (1972) Bussei Kenkyu 17: 282–286
[33] *Blachnik R, Gather B* (1983) J Less Common Metals 92: 207–213
[34] *Predel B, Piehl J, Pool MJ* (1975) Z Metallkunde 66: 347–352
[35] *Fuglevicz B* (1984) Polish J Chem 58: 983–984
[36] *Fujimoto M, Sato Y* (1966) Jpn J Appl Phys 5: 128–133
[37] *Brebrick RF, Strauss AK* (1964) J Chem Phys 40: 3430–3241
[38] *Bis RF* (1963) J Phys Chem Solids 24: 579–581
[39] *Gas'kov AM, Zlomanov VP, Novoselova AV* (1970) Vestn Mosk Univ Khim 25: 49–50
[40] *Zlomanov VP, Novozhilov AF, Novoselova AV, Makayov AV* (1977) Paluprovda. Materialy i Ikh Primenenie: 90–103
[41] *Sadykov KB, Semenkovich SA* (1966) Izvest Akad Nauk Turkm SSR, Ser Fiz Tekh Khim Geol Nauk 2: 16–21
[42] *Shamsuddin M* (1977) Mat Res Bull 12: 7–12
[43] *Sealy BJ, Crocker AJ* (1973) J Mater Sci 8: 1737–1743
[44] *Blachnik R, Igel R* (1974) Z Naturforsch 29 B: 625–629
[45] *Wohlrab M* (1966) Ann Physik (7) 17: 89–90
[46] *Blachnik R, Kluge W* (1972) Thermochem Acta 3: 317–325
[47] *Petukhov AP, Korner BF, Golovchenko VV* (1980) Izvest Akad Nauk SSSR, Neorg Mater 16: 358–359
[48] *Fabre C* (1887) Compt Rend 105: 277–280
[49] *Hirayama C* (1964) J Chem Eng Data 9: 65–68
[50] *Robinson PM, Bever MB* (1966) Trans TMS AIME 236: 814–817
[51] *Vecher AA, Mechkovskii LA, Skoropanov AS* (1974) Izvest Akad Nauk SSSR, Neorg Mater 10: 2140–2143
[52] *McAteer JH, Seltz H* (1936) Am Chem Soc 58: 2081–2084
[53] *Shamsuddin M, Misra S* (1981) In: *Gokcen NA* (ed) Chemistry metallurgy—a tribute to Carl Wagner, The Metallurgical Society of AIME, pp 241–256
[54] *Pashinkin AS, Novoselova AV* (1959) Russian J Inorg Chem 4: 1229–1231
[55] *Sokolov VV, Pashchinkin AS, Novogelova AV, Ryazantsev AA, Dolgikh VA, Klinchikova SA* (1969) Inorg Mater 5: 12–15
[56] *Mills KC* (1974) Thermodynamic data for inorganic sulfides, selenides and tellurides, Butterworth and Co.
[57] *Laugier A* (1973) Rev Phys Appl 8: 259–270
[58] *Laugier A, Cadoz J, Faure M, Moulin M* (1974) J Cryst Growth 21: 235–242
[59] *Szapiro S, Tamari N, Shtrikman H* (1981) J Electron Mater 10: 501–516
[60] *Kattner U, Lukas HL, Petzow G* (1986) Calphad 10: 103–116
[61] *Sharma RC, Chang YA* (1979) Metall Trans B 10B: 103–108
[62] *Sharma RC, Chang YA* (1980) Metall Trans B 11B: 139–146
[63] *Chuang Y-Y, Hsieh K-C, Chang YA* (1985) Metall Trans B 16B: 277–285
[64] *Hsieh K-C, Wei MS, Chang YA* (1983) Z Metallk 74: 330–337
[65] *Schmid R, Chang YA* (1985) Calphad 9: 363–382
[66] *Kellogg HH* (1976) In: *Fisher RM, Oriani RA, Turkdogan ET* (eds) Physical chemistry in metallurgy. US Steel Res Lab, Monroeville, PA, pp 49–68

[67] *Chuang Y-Y, Schmid R, Chang YA* (1984) Metall Trans A 15A: 1921–1930
[68] *Prigogine I, Defay O* (1965) Chemical thermodynamics. Longmans Green and Co., London, pp 410–411
[69] *Lupis CHP, Elliott JF* (1966) Acta Met 14: 529–538
[70] *Lin J-C, Ngai TL, Chang YA* (1986) Metall Trans A 17A: 1241–1245
[71] *Brebrick RF* (1977) J Electron Mater 6: 659–692
[72] *Hultgren R, Desai PD, Hawkins DT, Gleiser M, Kelley KK, Wagman DD* (1973) Selected values of the thermodynamic properties of the elements. Am Soc for Metals, Metals Park, Ohio
[73] Bulletin of Alloy Phase Diagrams (1981) 2: 146
[74] *Greenwood JN, Worner HW* (1939) J Inst Met 115: 435–445
[75] *Heinrich H* (1980) In: *Zawadzki W* (ed) Narrow gap semiconductors physics and applications. Springer, Berlin Heidelberg New York, p 407
[76] *Hemstreet LH* (1975) Phys Rev B 12: 1212
[77] *Chang YA* and co-workers (1986) unpublished data, University of Wisconsin-Madison, Madison, Wisconsin
[78] *Bhatia AB, Thornton DE* (1970) Phys Rev B 8: 3004–3012
[79] *Waseda Y, Jacob KT* (1981) Arch Eisenhüttenwes 52: 131–136
[80] *Hewes CR, Adler MS, Senturia SD* (1973) Phys Rev B 7: 5195
[81] *Preier H* (1979) Appl Phys 20: 189